On the applicability of empirical heat transfer models for hydrogen combustion engines

Demuynck, Joachim; De Paepe, Michel; Huisseune, Henk; Sierens, Roger; Vancoillie, Jeroen; Verhelst, Sebastian

In: INTERNATIONAL JOURNAL OF HYDROGEN ENERGY, 36 (1), 975-984, 2011

http://dx.doi.org/10.1016/j.ijhydene.2010.10.059

On the applicability of empirical heat transfer models for hydrogen combustion engines

J. Demuynck, M. De Paepe, H. Huisseune, R. Sierens, J. Vancoillie, S. Verhelst

Ghent University, Department of Flow, Heat and Combustion Mechanics,
Sint-Pietersnieuwstraat 41 B-9000 Gent, Belgium

Abstract

Hydrogen-fuelled internal combustion engines are being investigated as an alternative for current drive trains because they have a high efficiency, near-zero noxious and zero tailpipe greenhouse gas emissions. A thermodynamic model of the engine cycle would enable a cheap and fast optimization of engine settings for operation on hydrogen, facilitating the development of these engines. The accuracy of the heat transfer submodel within the thermodynamic model is important to simulate accurately the emissions of oxides of nitrogen which are influenced by the maximum gas temperature. These emissions can occur in hydrogen internal combustion engines at high loads and they are an important constraint for power and efficiency optimization. The most common heat transfer models in engine research are those from Annand and Woschni. These models are developed for fossil fuels, which have different combustion properties. Therefore, they need to be evaluated for hydrogen. We have measured the heat flux and the wall temperature in an engine that can run on hydrogen and methane. This paper describes an evaluation of the models of Annand and Woschni, using those heat flux measurements and assesses if the models capture the effect of changing combustion and fuel properties. The models fail on all the tests, so they need to be improved to accurately model the heat transfer generated by hydrogen combustion.

Keywords: hydrogen, methane, internal combustion engine, experimental, heat transfer, model

Nomenclature

Abbreviations

°CA	degree crank angle
NO_x	oxides of nitrogen
ABDC	after bottom dead centre
ATDC	after top dead centre
BBDC	before bottom dead centre

*Corresponding author. Tel.: +32(0)92643302; Fax: +32(0)92643590
Email address: joachim.demuynck@ugent.be (J. Demuynck)

BTDC before top dead centre

CFR Cooperative Fuel Research

EGR exhaust gas recirculation

EVC exhaust valve closure

EVO exhaust valve opening

FS full scale

GUEST Ghent University engine simulation tool

HFM heat flux microsensor

HFS heat flux sensor

IGN ignition timing

IMEP indicated mean effective pressure

IVC intake valve closure

IVO intake valve opening

MBT minimum spark advance for maximum brake torque

PFI port fuel injection

RTD resistance temperature detector

RTS resistance temperature sensing

SA sample signal

TRIG trigger signal

WOT wide-open-throttle

Greek symbols

α thermal diffusivity, $\left[m^2/s\right]$

ϵ compression ratio

λ air-to-fuel equivalence ratio

ν kinematic viscosity, $\left[m^2/s\right]$

Roman Symbols

c_m average piston speed, $[m/s]$

D cylinder bore, $[m]$

h convection coefficient, $\left[W/(m^2 \cdot K)\right]$

k thermal conductivity, $[W/(m \cdot K)]$

L characteristic length, $[m]$

Nu Nusselt number

Pr Prandtl number

q heat flux, $\left[W/cm^2\right]$

q_{max} maximum heat flux

Q_h total cycle heat loss, $[J]$

Re Reynolds number

T_g gas temperature, [°C]

T_w wall temperature, [°C]

V characteristic velocity, $[m/s]$

V_c in-cylinder volume, $\left[m^3\right]$

W_i indicated work, $[J]$

1. Introduction

Many alternative fuels are being put forward to replace the fossil fuels. However, there is no silver bullet, so several promising fuels are examined at the Transportation Technology research group of Ghent University. Research for road transport is focused on hydrogen and methanol [1]. Pure vegetable oils, animal fats and residual products are explored for stationary and medium speed diesel engines [2, 3, 4].

This paper is related with the investigation of the hydrogen-fuelled combustion engine. Hydrogen is an energy carrier with large potential if it is produced with renewable energy sources [5, 6]. Research has proven that the combustion properties of hydrogen enable an engine with a high efficiency and a wide range of operational strategies [7]. Moreover, hydrogen engines have near-zero noxious and zero greenhouse gas emissions which makes them an attractive alternative for the current drive trains. The initial research at Ghent University focused on the experimental optimization of engine operational strategies for maximum power and efficiency, with ultra low emissions of oxides of nitrogen (NO_x) [8, 9, 10, 11]. This focus shifted to numerical research with the development of a thermodynamic model of the engine cycle, the GUEST-code (Ghent University Engine Simulation Tool) [12].

Such a thermodynamic model of the engine cycle enables a cheap and fast optimization of engine settings for operation on hydrogen. Within the cycle model, several sub models are necessary to solve the conservation equations of energy and mass: a combustion, a turbulence and a heat transfer model among other things. The last one is important to simulate accurately the emissions of oxides of nitrogen which are influenced by the maximum gas temperature. These emissions can occur in hydrogen internal combustion engines at high loads, being an important constraint for power and efficiency optimization.

Several heat transfer models for internal combustion engines exist in the literature. The review described below will show that the models of Annand [13] and Woschni [14] are mostly used, but they are developed for fossil-fuelled engines. This paper will show that the heat transfer process of hydrogen differs a lot compared to that of a fossil fuel, in this case methane, so the models have to be evaluated for hydrogen.

In a previous paper, we reported heat transfer and wall temperature measurements in a spark ignited engine with a commercially available heat flux sensor [15]. Here, we describe the evaluation of the heat transfer models of Annand and Woschni with those measurements. The simulation results are evaluated based on two criteria: the maximum in the heat flux trace (q_{max}) and the total cycle heat loss (Q_h). It is important that the models perform well on both values. The maximum heat flux has an influence on the maximum gas temperature, hence an accurate prediction of it is important for a good determination of NO_x emissions. An accurate estimation of the total cycle heat loss is important for a correct calculation of the engine's power and efficiency. Below, a description of the experimental method and an overview of the existing heat transfer models are given, before describing the results of the models' evaluation.

2. Experimental method

2.1. Equipment

A CFR (Cooperative Fuel Research) engine [16] is used for the research. The engine is operated at a constant speed of 600 rpm and is equipped with one gas injector in the intake manifold (PFI: port fuel injection) that can be used for the injection of hydrogen or methane. The engine has a variable compression ratio, which is kept below 10 because the heat flux sensor would be covered by the piston around TDC (top dead centre) at higher compression ratios. The details of the engine are given in Table 1. The engine's liner and head are one piece, made out of cast iron. The piston is made out of cast iron as well and contains 5 piston rings. Fuel injection and ignition timing (IGN) are controlled by a *MoTeC M4Pro* electronic control unit. The injection pressure is 2 bar and the end of the injection is always at BDC (Bottom Dead Centre) of the induction stroke. The ignition timing is always at MBT (minimum spark advance for Maximum Brake Torque).

The measurements were carried out with a *Vatell HFM-7* sensor which consists of a thermopile (heat flux signal, HFS) and an RTD (substrate temperature signal, RTS). Vatell claims that the sensor has a response time of 17 µs. The *Vatell AMP-6* amplifier was used as a current source for the RTD and as an amplifier for both output signals. As the test engine is easily accessible, the heat flux sensor was successively installed

in three different positions under fired operation (P2, P3, P4 as shown in Fig. 1). These openings are at the same height in the cylinder wall and are equally distributed around the circumference of the cylinder. The spark plug was placed in position P1. The heat flux sensor could be mounted in P1 as well in the case of motored operation, because of the absence of the spark plug. The heat flux of all the measurement positions is averaged for the evaluation of the models, since they predict a spatially averaged heat flux.

In-cylinder and inlet pressure were measured with a water-cooled *Kistler 701A* piezoelectric (in P2 or P4) and *Kistler 4075A20* piezoresistive pressure sensor, respectively. The inlet pressure was used to reference in-cylinder pressure. A 12 bit data acquisition card was used to sample both the heat flux and pressure signals. It is triggered by a crank angle encoder every 0.5 °CA, resulting in a sampling rate of 7.2 kHz. Gas flows were measured with *Bronkhorst Hi-Tec F-201AC* (fuel) and *F-106BZ* (air) flow sensors. Finally, type K thermocouples were used to measure inlet and exhaust gas temperatures.

The total cycle heat loss (Q_h) is estimated, assuming that the average of the measured heat flux traces occur evenly over the entire cylinder wall. The average of the measured heat fluxes is multiplied with the total available in-cylinder surface for each sampling point and all these values are summed up to get the total cycle heat loss. Q_h is limited to the zone between IVC and EVO to be comparable with the simulation results.

2.2. Error analysis

To judge the quality of the measurement results, a thorough error analysis has been carried out following the methods described in Taylor [17]. The error analysis is based on the accuracy of the measurement equipment which is given in Table 2. The pressure measurement circuit was calibrated with a dead-weight tester in the laboratory. The given uncertainty of a pressure sensor is the standard deviation of the calibration which is repeated 50 times. The HFM sensor is not included in Table 2 because its accuracy depends on several coefficients which are used to calculate the heat flux and wall temperature out of the measured HFS and RTS signal (see HFM manual [18]). These coefficients and their uncertainty are determined during the calibration of the sensor at the factory of Vatell. The resulting maximum relative errors on the measured and calculated variables are given in Table 3. The uncertainty on the compression ratio (ϵ) and specific gas constant (R) are negligible.

The uncertainty on the convection coefficient is calculated assuming that the in-cylinder temperature at EVC is equal to the exhaust temperature as explained in Appendix A. A sensitivity analysis has been performed to check the influence of this choice. Varying the cylinder temperature at EVC with 20 % changes the residual gas fraction with 10 %, but the calculated bulk gas temperature and convection coefficient only change with 1 %. This influence is acceptable for the calculations in this paper.

3. Hydrogen vs. methane

We have demonstrated before that the heat transfer caused by hydrogen combustion differs a lot from that caused by methane combustion [15, 19]. Here, we show this with

a comparison between both fuels at two engine power outputs to highlight the need for the evaluation of the existing heat transfer models. The heat flux generated by the combustion of the two fuels is each time compared at the same engine load. However, there is a difference in the way the engine is operated. For hydrogen, the air-to-fuel equivalence ratio (λ) is varied at wide-open-throttle (WOT). For methane, the mixture richness cannot be varied in a wide range. Therefore, a throttle had to be used in the intake manifold to vary the power output, keeping λ equal to 1. The imep (indicated mean effective pressure) of the low load is equal to 4.7 bar, that of the high load is 6.1 bar. The comparison described below is for a compression ratio of 8, but similar results are observed for the other compression ratios.

The heat flux traces for the two loads are plotted in Fig. 2, those of hydrogen with a solid line and those of methane with a dotted line. The initial rise in the heat flux traces is caused by the flame passage over the measurement position. Although the flame speed is slower for the leanest hydrogen measurement (black colour), the initial rise occurs a little bit earlier than that of the stoichiometric measurement (red colour) due to the advanced ignition timing. The fast and short combustion of the stoichiometric hydrogen mixture generates a high peak in the heat flux trace. This peak greatly reduces with a decreasing mixture richness. A reduction of 80 % is noticed if λ is changed from 1 to 2. The resulting power output decreased with 23 %. In contrast, the heat flux traces of methane remain almost the same. Reducing the in-cylinder mass has a large effect on the resulting power output, but not on the heat transfer. The heat transfer does decrease when the load is reduced, but not as much as expected due to the extra turbulence generated by the throttle. The mixture richness on the other hand has a great influence on the heat transfer process. The peak in the stoichiometric heat flux trace of hydrogen is 3 times higher compared to methane, but it is lower if λ is equal to 2. Figure 2 clearly demonstrates that there is a difference in the heat transfer process between hydrogen and a fossil fuel, so the existing heat transfer models need to be evaluated for hydrogen.

4. Existing heat transfer models

This section gives an overview of the heat transfer models in the literature. The goal of this paper is to evaluate the heat transfer models that can be plugged into the GUEST code. Therefore, only models that calculate an instantaneous, spatially averaged heat flux (q) as a function of the crank position are discussed. The purpose of the heat transfer model is to predict the total amount of heat that is lost to the cylinder walls during each time step of the engine cycle calculation. This amount of heat is needed to solve the conservation equation of energy. Moreover, the focus is on the convective part of the heat transfer models, because spark ignition engines are the aim and radiation is only significant in diesel engines [20]. All the models discussed below, assume that the heat transfer process in an engine is quasi-steady. Then, the convective component can be described by a convection coefficient (h), defined in equation 1. The model of Kleinschmidt [21], which expands the theories of Pfriem [22] and Elser [23], is not based on the quasi-steady assumption. However, this model is not evaluated here, since it is not directly suitable for the GUEST code.

$$q = h \cdot \Delta T \tag{1}$$

Where ΔT is the difference between the wall temperature (T_w) and the bulk gas temperature (T_g).

Annand [13] was the first to gather the research on heat transfer that was done until the early sixties. He reviewed the existing models for engine heat transfer, stating that they were dimensionally inconsistent. To solve this, he modelled the convective part of the heat transfer based on the boundary layer theory, which describes the heat transfer caused by a flow over a flat plate. The heat transfer is represented by the Nusselt number ($= h \cdot L/k$) as a function of the Reynolds ($= V \cdot L/\nu$) and Prandtl ($= \alpha/\nu$) number, shown in equation 2.

$$Nu = a \cdot Re^b \cdot Pr^c \tag{2}$$

There are three important remarks about the application of the equation given above. First, the Prandtl number is almost constant and around 0.7 for all the gases (except H_2O) so Annand included it into the parameter a to reduce calculation efforts. Second, Annand suggested to evaluate gas properties at the calculated gas temperature (T_g) instead of defining a temperature between T_g and T_w, because T_g is already an average gas temperature. Ultimately, a characteristic length (L) and velocity (V) have to be defined for the calculation of the Nusselt and Reynolds number. Annand used the cylinder bore (D) and the mean piston speed (c_m), respectively.

The heat flux to the cylinder walls can be derived if equations 2 and 1 are combined into equation 3.

$$q_{convective} = \frac{a \cdot k}{D} \cdot Re^b \cdot (T_g - T_w) \tag{3}$$

Annand fitted the model to the available heat transfer measurements at that time and concluded that the parameter a should have a value between 0.35 and 0.8 and that b should be equal to 0.7. Parameter a depends on the engine geometry and charge motion. Therefore, it can be used as a scaling factor to fit the model to a certain engine. Annand and Ma [24] tried to improve the first model of Annand, but could not prove that with their measurements in a diesel engine. Therefore, the first model of Annand has been used ever since.

A second widely used model is that of Woschni [14], who followed Annand and based his model on equation 2, with the Prandtl number lumped into a. There are three main differences between the models of Woschni and Annand.

First, Woschni took a from models which describe the heat transfer of flows in tubes ($a = 0.045$), being an order of magnitude lower compared to that of Annand. Second, he converted equations 1 and 2 into equation 4 (as described in [25]) in order to calculate the heat flux as a function of only the cylinder bore, the characteristic velocity, the pressure and the temperature. Therefore, he made the following assumptions:

- $b = 0.8$
- $\rho \sim p/T$
- $k \sim T^{0.75}$

- $\mu \sim T^{0.62}$

$$q = a_{Wo} \cdot D^{-0.2} \cdot p^{0.8} \cdot V^{0.8} \cdot T^{-0.53} \cdot (T_g - T_w) \tag{4}$$

Due to the assumptions, the parameter in front of the equation is not dimensionless anymore. Its dimensions and value if Woschni's or SI units are used are given in equation 5.

$$a_{Wo} = 110, \left[\frac{kcal}{h} \cdot \left(\frac{kp}{cm^2} \right)^{0.8} \cdot \frac{s^{0.8}}{m^{2.6}} \cdot K^{0.47} \right] \tag{5a}$$

$$a_{Wo,SI} = 0.012991, \left[W \cdot Pa^{0.8} \cdot \frac{s^{0.8}}{m^{2.6}} \cdot K^{0.47} \right] \tag{5b}$$

Third, Woschni stated that the characteristic velocity has to have an additional term representing the effect of the combustion on the heat transfer. Therefore, he added the pressure difference between the fired and the motored case. The resulting characteristic velocity is given in equation 6.

$$V = c_1 \cdot c_m + c_2 \cdot \frac{V_s \cdot T_r}{p_r \cdot V_r} \cdot (p - p_0) \tag{6}$$

With:

- $c_1 = 6.18$ during the scavenging period and $c_1 = 2.28$ during the compression, combustion and expansion period
- $c_2 = 0$ during the scavenging and compression period and $c_2 = 3.24 \cdot 10^{-3}$ during the combustion and expansion period, $[m/s^{\circ}\mathrm{C}]$
- subscript r denotes a reference state where volume, pressure and temperature are known
- p_0 is the in-cylinder pressure under motored conditions

The last two assumptions that Woschni made in the derivation of equation 4 are only valid for air, so the extrapolation of the model to other gases is actually not justified. There are other models in the literature (e.g. references [26, 27, 28]) which are derived from equation 4. However, these are not evaluated here, because their exponents of pressure and temperature have been tuned to be valid for a certain measurement set. Consequently, there is no link anymore with equation 2 and the extrapolation to other engines is expected to be worse.

Shudo and Suzuki [29] and Nefischer et al. [30] suggested new models for hydrogen engines. Shudo and Suzuki based their model on that of Woschni and changed the second term in equation 6 into a rate of heat release. That model is not considered to be an improvement, because of the remark given above about the models derived from Woschni and the fact that they needed to recalibrate their model for every measurement in order to match the measured heat flux. The model of Nefischer et al. predicts a

local heat flux and is not directly suitable for GUEST. Therefore, these models are not evaluated in this paper.

Because the calculation of a Prandtl number is computationally not a problem anymore, it is not included in the coefficient a for the model of Annand and a coefficient c of $1/3$ is used, according to the boundary layer theory. The heat fluxes are only simulated between IVC (intake valve closure) and EVO (exhaust valve opening). The calculation of the variables that have to be filled into equations 3 and 4 are given in Appendix A.

It is important to state that the models are very sensitive to a change in the calibration constants. A change of 20 % in a results in a change of 20 % in the predicted heat transfer of the model of Annand. The model of Woschni is less sensitive to c_1 and c_2 during the combustion period. Changing one of the calibration constants with 20 % results in a change of around 10 % in the predicted heat flux, demonstrating that both parts of equation 6 are of equal magnitude. Woschni's model will be more sensitive to c_1 at higher engine speeds, because c_m will be higher.

5. Results and discussion

The aforementioned parameters in the models have to be tuned to calibrate the models for the geometry of the investigated engine. The number of required calibrations will be tested in order to assess the accuracy of the models. The operational conditions of the measurements used for the evaluation of the models are given in Table 4. The ones in bold are the reference measurements used for the calibration of the models (see below).

5.1. Motoring operation

First, the models are calibrated for a reference measurement under motored operation and they are evaluated for a variation in the compression ratio and the throttle position. The measurement with a compression ratio of 8 is used as the reference case. The parameters of the models are tuned so that the models predict correctly the peak value of the heat flux trace. The resulting parameter a in the model of Annand, is equal to 0.265, which is below the minimum suggested value of 0.35. The parameter c_1 in the model of Woschni has to be 2.7, which is the same order of magnitude as the suggested value of 2.28. The parameter c_2 is not fixed yet, because this represents the influence of the combustion which is not present under motored operation. These values of the coefficients are now fixed for the other simulations to check how accurate the models simulate a variation in the compression ratio and the throttle position.

The simulation results for a compression ratio between 6 and 10 are compared with the measured heat flux traces in Fig. 3. Those for a variance in the throttle position are plotted in Fig. 4. Throughout the entire paper, the measured heat flux traces are plotted with a solid line and the simulations with two different styles of a dotted line. The numerical values of the measured q_{max} and Q_h are given in Table 5 together with the relative errors of the models' predictions. The measurement numbers in that table are the same as the ones defined in Table 4.

Both models can predict the increasing trend in the heat flux with an increasing compression ratio, since the relative error on the simulated results is close to the measurement uncertainty of the heat flux. The models predict a lower heat flux during the compression stroke and a higher one during the expansion stroke. This leads to relative errors on the predicted Q_h between 15 and 35 %, which are no longer within the measurement uncertainty. There is no significant difference between the predictions of the two models. This is an expected result because the assumptions made by Woschni are valid for air, so only the exponent b is different.

Two different throttle positions are tested. Position 1 and 2 reduce the intake air flow rate compared to WOT with 50 and 75 %, respectively. The plot in Fig. 4, where T pos stands for throttle position, shows that the two models fail to predict a change in the throttle position. They predict the decreasing trend with smaller throttle opening, but they overestimate its effect. The experimental heat flux trace drops faster after TDC. Consequently, the models significantly over predict the heat transfer during the expansion stroke, leading to large relative errors on Q_h (see Table 5).

5.2. Fired operation - methane

Next, the hypothesis that the models have to be calibrated only once for a certain engine will be tested by evaluating their predictions for methane combustion. This hypothesis only applies to the model of Annand, since that of Woschni can be calibrated separately for the fired conditions because of the term in the characteristic velocity representing the influence of the combustion process. The models are first evaluated for methane combustion, because this represents a fossil fuel for which they have been developed. Annand's simulation result for a stoichiometric-WOT-measurement, plotted in Fig. 5, is significantly too low. Consequently, the hypothesis is rejected and the model of Annand has to be recalibrated for methane which results in an a of 0.44 (in the range suggested by Annand). Fig. 5 shows that c_2 in Woschni's model has to be equal to $4.3 \cdot 10^{-3}$, which is the same order of magnitude of the suggested value of $3.24 \cdot 10^{-3}$.

The heat flux traces in Fig. 5 show that the model of Annand overestimates the heat flux at the end of the compression and expansion stroke. This is not the case for the simulation result with the lower value for a (for the motored measurements), so it demonstrates that the parameter a had to be set too high. The model of Woschni is able to predict more accurately the heat flux during the entire engine cycle. This shows that there is an influence of the combustion process on the heat transfer which cannot be predicted by a constant characteristic velocity.

5.3. Fired operation - hydrogen

Now, the hypothesis that the models incorporate the effect of the fuel properties is tested. The measurement and simulations of the heat flux for hydrogen combustion (with a λ of 1.5) are plotted in Fig. 6. The plot shows that the models do not accurately simulate the heat flux of hydrogen combustion at all, if the parameters are kept constant ($a = 0.44$, $c_1 = 2.7$ and $c_2 = 4.3 \cdot 10^{-3}$), and the hypothesis can be rejected. The maximum heat flux is simulated with an error of 117 % in the case of the model of Woschni and 96 % in the case of the model of Annand. The heat flux traces in Fig. 6 between

270 and 360 °CA show that the model of Annand better predicts the heat transfer during the compression stroke than the model of Woschni. The model of Woschni under predicts the heat flux there, which was not the case for the methane measurement. This demonstrates that it is better to calculate the gas properties instead of using assumptions which are only valid for air, especially when dealing with hydrogen. This seems obvious, but it has been overlooked by many authors who build upon the model of Woschni for fossil fuels [26, 27, 28] or hydrogen [29].

Next, the models are recalibrated for the hydrogen measurement discussed above and their ability to predict the effect of a variance in the air-to-fuel equivalence ratio is assessed (see Fig. 7). The parameter a in equation 3 has to be set to 0.87 and c_2 in equation 6 has to be set to $1.7 \cdot 10^{-2}$. These values are outside the expected range for the parameters, confirming the previous statement that the models are not appropriate for hydrogen. The measured values for q_{max} and Q_h are given in Table 6 together with the relative errors of the models' predictions.

Again, the model of Annand predicts a heat transfer which is too high during the compression and expansion stroke. Consequently, the error on the predicted value of Q_h for the reference measurement is significantly higher compared to that of Woschni. The experimental heat flux traces showed a 79 % decrease in the peak of the heat flux if the mixture richness was decreased from $\lambda = 1$ to $\lambda = 2$. Woschni's model predicts a 68 % decrease and Annand's model only a 51 % decrease. Clearly, both models do not simulate well the trend for a decreasing mixture richness, since all the errors on the simulation results are significantly higher than the measurement errors. The prediction of Woschni's model is closer to the measurement, because it incorporates the effect of the cylinder pressure (see equation 6).

The models clearly lack some variables that have an influence on the heat transfer process in hydrogen engines. It is believed in literature that there are three reasons for the difference in the heat transfer of hydrogen compared to a fossil fuel: the higher thermal conductivity, the faster flame velocity and the smaller quenching distance. The effect of the thermal conductivity is captured by the model of Annand. Therefore, the main lacking parameters are probably the influence of the faster combustion process and the shorter quenching distance. This will be investigated more elaborately in future research.

Ultimately, a combination of the two models is tested, since it might be better to use the model of Annand (equation 2) as a basis with the characteristic velocity of Woschni (equation 6) plugged into it. Figure 8 shows the reference measurement for hydrogen with the prediction results of the model of Annand (with $a = 0.44$) and that of the combination model (AnWo). In that combination model, a is set equal to 1 and c_1 is calibrated for the reference measurement under motored conditions, being equal to 0.15 ($= 0.265^{-0.7}$). c_2 is calibrated for the methane measurement and has to be equal to $1.6 \cdot 10^{-4}$. The plot shows that this combination of the models is not sufficient either. The accurate prediction result of Annand's model near the end of the compression stroke for hydrogen in Fig. 6 was due to the fact that a was set too high to match the peak of the methane measurement, instead of capturing the effect of the change in fuel. However, the statement about the calculation of the gas properties remains valid.

6. Conclusions

The heat transfer models of Annand and Woschni are still the most used ones for internal combustion engine research. They have been developed a long time ago for fossil fuels and they have to be evaluated for alternative fuels that are investigated these days. One of the fuels that is investigated at Ghent University is hydrogen. This paper has demonstrated that the heat transfer process of this fuel differs a lot from a fossil fuel (methane) and has described an evaluation of those models with heat transfer measurements in a spark ignition engine under motored and fired operation.

It has been demonstrated that the heat flux in a combustion engine cannot be modelled with a constant characteristic velocity and that it is better to calculate the gas properties instead of using the assumptions of Woschni. Several hypotheses regarding the amount of necessary calibrations were tested. First, the models have been calibrated for a measurement under motored operation to account for the influence of the specific engine geometry. Both models were able to simulate the increasing trend in the maximum heat flux with an increasing compression ratio. In contrast, the simulation results of the total cycle heat loss and the variation in throttle position were less accurate. Then, the hypothesis that the models only have to be calibrated once for a certain engine was rejected by evaluating them for methane. Next, the hypothesis that the models incorporate the effect of the fuel properties was rejected by evaluating them for hydrogen. Ultimately, after a recalibration for hydrogen, the models were also not able to predict accurately the trends for a variation in the equivalence ratio.

Clearly, the models lack some parameters that have an influence on the heat transfer process in an engine. Therefore, they have to be recalibrated every time and need to be improved. For hydrogen, they are not even capable of simulating a variance in the air-to-fuel equivalence ratio after a calibration.

Table 1: Geometrical properties and valve timing of the CFR engine

Bore	82.55 mm
Stroke	114.2 mm
Connecting rod length	254 mm
Swept volume	611.7 cm^3
IVO	17 °CA ATDC
IVC	26 °CA ABDC
EVO	32 °CA BBDC
EVC	6 °CA ATDC

Table 2: The accuracy of the measurement equipment

Variable	Device	Accuracy
Heat flux gain	Vatell AMP-6	±3.6%
Wall temperature gain	Vatell AMP-6	±1.5%
In-cylinder pressure	Kistler 701A	±1%
Intake manifold pressure	Kistler 4075A20	±2.5%
Air flow rate	Bronkhorst F-106BZ	$\pm 1\% FS$
Hydrogen flow rate	Bronkhorst F-201AC	$\pm 1\% FS$
Engine speed	ASTM tachometer	±6 rpm
Atmospheric temperature		±0.5 °C
Atmospheric pressure		±50 Pa

Table 3: The maximum relative errors on the measured and calculated variables

Variable	Symbol	Accuracy
Heat flux (during the compression and expansion stroke)	q	±3%
Heat flux (during the intake and exhaust stroke)	q	±7%
Wall temperature	T_w	±5%
Gas temperature	T_g	±6%
In-cylinder volume	V_c	±1%
Air and hydrogen flow rate	-	±4%
Methane flow rate	-	±9%
Hydrogen air-to-fuel equivalence ratio	λ	±5%
Methane air-to-fuel equivalence ratio	λ	±10%
Indicated Work output	W_i	±2.5%
Total cycle heat loss	Q_h	±7.6%
Convection coefficient	h	±11%

Table 4: Overview of the measurements used for the evaluation

measurement	operation	fuel	ϵ	throttle	λ	IGN (MBT)
1	motored	only air	6	WOT	-	-
2	**motored**	**only air**	**8**	**WOT**	**-**	**-**
3	motored	only air	8	pos. 1	-	-
4	motored	only air	8	pos. 2	-	-
5	motored	only air	10	WOT	-	-
6	fired	methane	8	WOT	1	30 °CA BTDC
7	fired	hydrogen	8	WOT	2	4 °CA BTDC
8	**fired**	**hydrogen**	**8**	**WOT**	**1.5**	2 °CA ATDC
9	fired	hydrogen	8	WOT	1	6 °CA ATDC

Table 5: Overview of the simulations' accuracy for motored operation

measurement	$q_{max,exp}$ (W/cm^2)	Annand	Woschni	$Q_{h,exp}$ (J)	Annand	Woschni
1	6.0	−2.5 %	−4.5 %	16.7	+34.8 %	+28.6 %
2	**8.8**	**0** %	**0** %	**21.9**	+**21.5** %	+**18.4** %
3	8.0	−13.9 %	−16.7 %	20.2	+7.7 %	+1.1 %
4	4.7	−13.2 %	−19.6 %	8.1	+35.7 %	+23.9 %
5	12.0	−5.0 %	−3.2 %	26.0	+16.5 %	+15.2 %

Table 6: Overview of the simulations' accuracy for fired operation

measurement	$q_{max,exp}$ (W/cm^2)	Annand	Woschni	$Q_{h,exp}$ (J)	Annand	Woschni
7	82.2	+59.6 %	+28.39 %	196.0	+134.6 %	+13.4 %
8	**188.2**	**0** %	**0** %	**311.8**	**+75.12** %	**−6.0** %
9	382.2	−30.5 %	−15.0 %	577.2	+21.3 %	−26.0 %

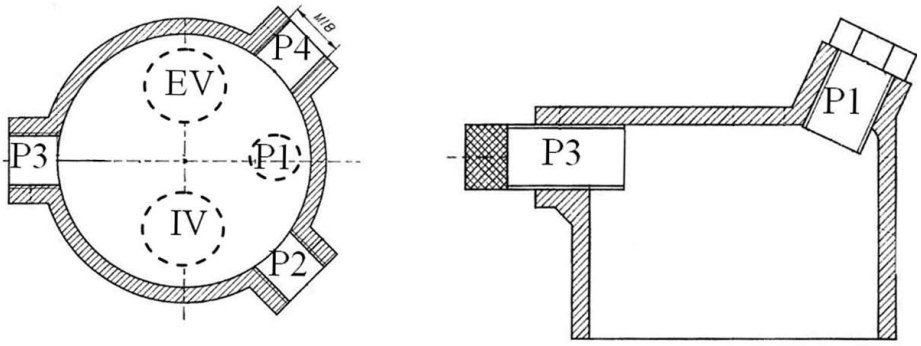

Figure 1: Cross-section of the CFR engine, P1: spark plug, P1-P4: sensor positions, IV: intake valve, EV: exhaust valve

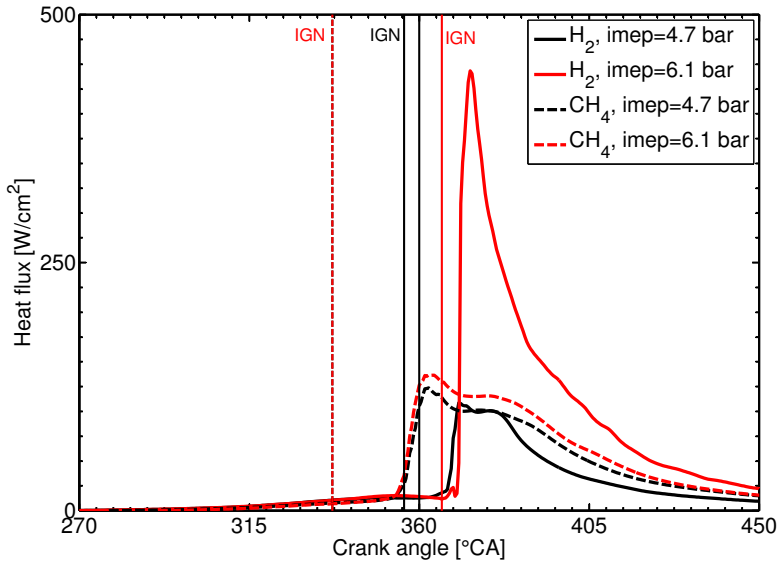

Figure 2: The heat transfer process of hydrogen differs significantly from that of methane

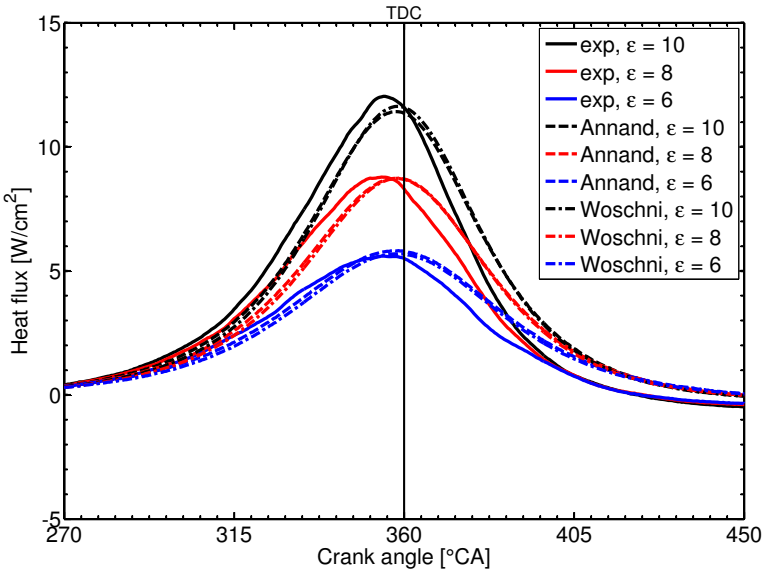

Figure 3: The heat transfer models can predict the trends for varying compression ratio under motored conditions (measurements 1-2-5)

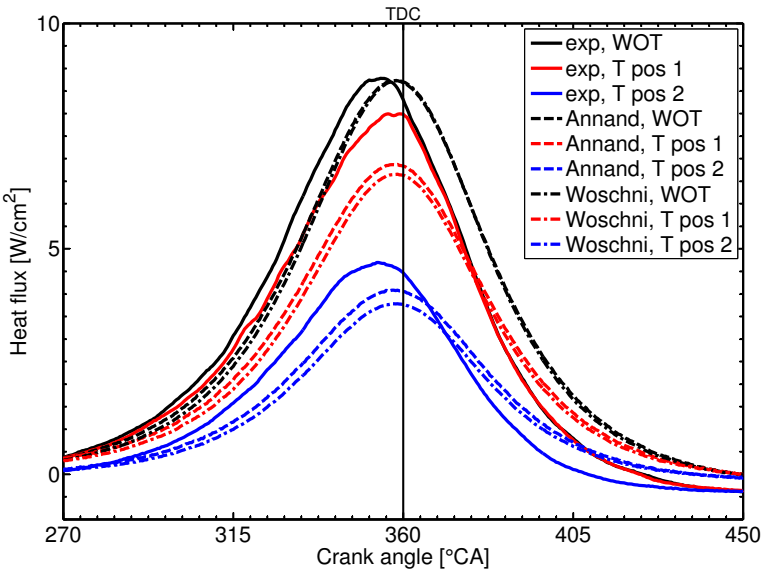

Figure 4: The heat transfer models predict the trends for a variation in the throttle position (T pos), but overestimate its effect. Throttle position 1 and 2 reduce the air flow rate with 50 and 75 %, respectively (measurements 2-3-4).

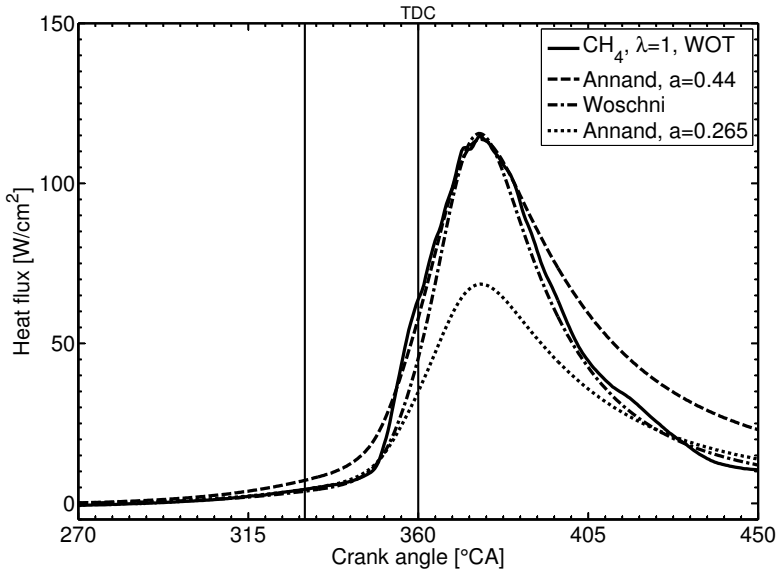

Figure 5: The model of Woschni can predict the heat transfer for methane combustion better than the model of Annand, because it has a second parameter that can be tuned (measurement 6)

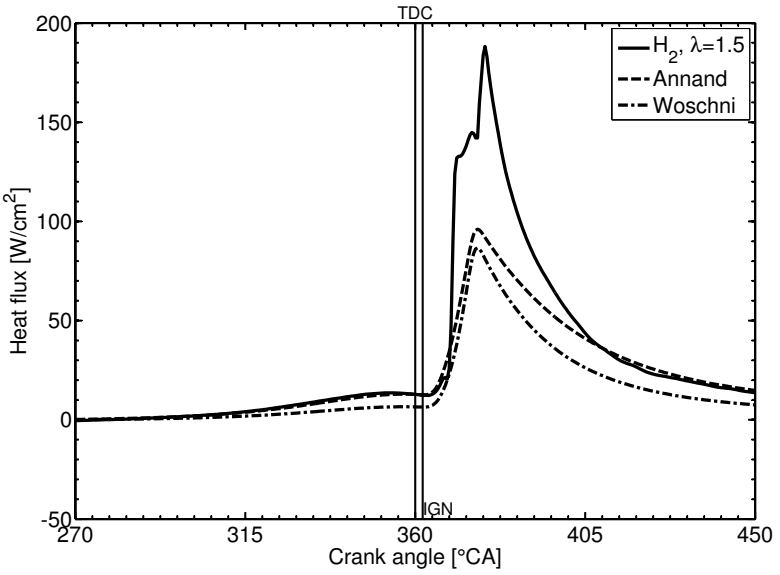

Figure 6: The heat transfer models fail in the prediction of the heat transfer of hydrogen combustion with the calibration settings for methane (measurement 8)

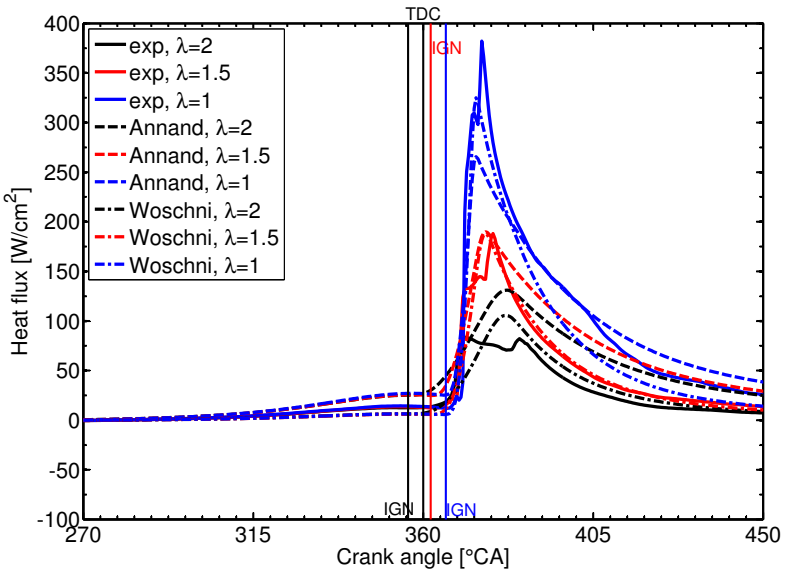

Figure 7: The models' parameters have to be too high if the models are recalibrated for hydrogen. The decreasing trend in the heat flux with decreasing mixture richness is predicted, but not accurately enough (measurements 7-8-9).

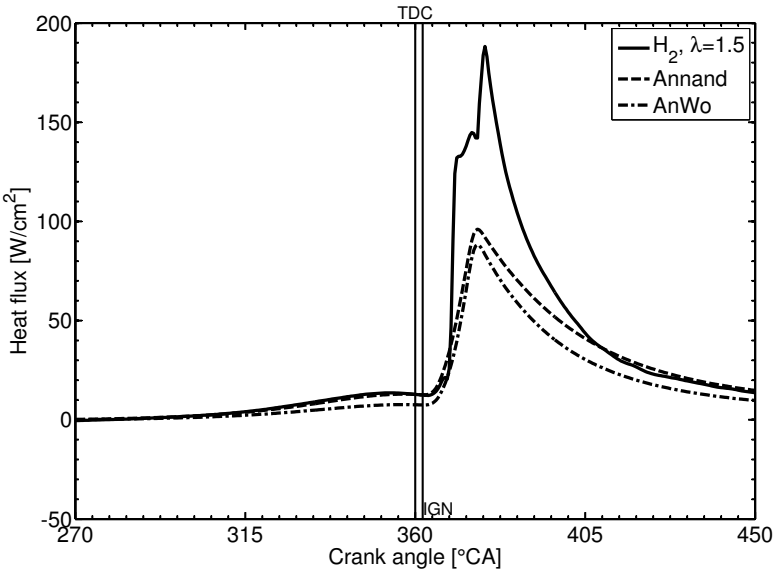

Figure 8: A combination of the models of Annand and Woschni is not able to simulate the heat transfer of hydrogen either (measurement 8)

Appendix A.

This appendix describes the calculation of the variables that have to be filled into equations 3 and 4. First, the difference between the bulk gas temperature and wall temperature has to be known in both heat transfer models. The wall temperature that is used, is the average of the measured ones at the three sensor locations, which differ between 10 and 20 °C. The combustion gases are assumed to behave like ideal gases. Therefore, the bulk gas temperature is calculated with the following equation of state: $T_g = p \cdot V_c / m \cdot R$.

- The in-cylinder pressure (p) is measured and the volume (V_c) can be calculated out of the crank position.
- The mass (m) can only be determined during the closed part of the combustion cycle, being the sum of the measured incoming mass (air and fuel) and the residuals. No incoming mass goes directly to the exhaust manifold because the test engine does not have a valve overlap. Consequently, the residual mass can be determined with the equation of state at EVC (exhaust valve closure), using the measured cylinder pressure and assuming that the in-cylinder temperature is equal to the measured exhaust temperature. Blow-by effects can be neglected because of the large number of piston rings (5).
- The specific gas constant (R) at IVC can be calculated out of the mass average of the specific gas constants of the air, the fuel and the residual gases. This value is used until the beginning of the combustion. At the end of the combustion, R is equal to that of the combustion products. In between, the specific gas constant is calculated with a linear interpolation. The instant where the combustion begins and ends is determined with a rate of heat release analysis.

The thermal conductivity, kinematic viscosity and Prandtl number of the gas mixture have to be calculated at each instant for the model of Annand. The heat capacity and the dynamic viscosity are calculated on top of the thermal conductivity to determine the Prandtl number. These variables are all calculated as a function of the gas temperature in the same way as the specific gas constant (three zones: between IVC and beginning of the combustion, during the combustion and during the expansion period), using the mixing rules described in [31]. For the heat capacity and the dynamic viscosity, the polynomials of the GUEST code [12] are used. New polynomials needed to be determined for the thermal conductivity because gas temperatures until 2500 K were noted, which is outside their validity range. A literature review did not reveal any data for such temperatures for all the gases. Therefore, the polynomials (4th order) are determined based on the data generated with the method of Chung et al., described in [31]. This method allows the calculation of the thermal conductivity out of available data for the heat capacity and the dynamic viscosity. The results of this method were checked against the polynomials in the GUEST code (within their validity range). The comparison showed that the results of the calculation method were within 5-8 % of the other data, which is acceptable. Only for water vapor the calculation results differed up

to 30 %. Therefore, the data of the International Association for the Properties of Water and Steam (IAPWS [32], valid until 1073 K) is used and extrapolated until 1600 K, where it coincides with the results of the method of Chung et al.

Woschni has converted the equation of the boundary layer theory so that it is only a function of pressure and temperature (besides the characteristic length and velocity). Consequently, it needs less data input. The measured cylinder pressure for the fired and motored case have to be filled in. IVC is taken as the reference state in the calculation of the characteristic velocity.

Acknowledgements

The authors of this paper like to acknowledge the suggestions and technical assistance of Koen Chielens and Patrick De Pue. The research is carried out in the framework of Ph.D.'s which are funded by the Institute for the Promotion of Innovation through Science and Technology in Flanders (IWT-Vlaanderen, SB-81139) and by the Research Foundation - Flanders (FWO, 09/ASP/030). The Research Foundation - Flanders (FWO) has also funded the experimental equipment (1.5.147.10N). These financial supports are gratefully acknowledged.

References

[1] J. Vancoillie, S. Verhelst, Modeling the combustion of light alcohols in SI engines: a preliminary study, in: Proceedings of the 2010 FISITA World Automotive Congress, Student Congress (F2010-SC-O-04), Budapest, Hungary, 2010.

[2] I. Mormino, S. Verhelst, R. Sierens, C. Stevens, B. Meulenaer, Using vegetable oils and animal fats in diesel engines: Chemical analyses and engine tests, SAE Paper 2009-01-0493 (2009).

[3] J. Galle, S. Verhelst, R. Sierens, L. Goyos, R. Castaneda, M. Verhaege, L. Vervaeke, M. Bastiaen, Failure of fuel injectors in a medium speed diesel engine operation on bio-oil, submitted to Biomass and Bioenergy.

[4] S. Verhelst, R. Sierens, L. Vervaeke, T. Berckmoes, L. Duyck, Medium speed diesel engines operated on alternative fuels: lessons learned and remaining questions, in: Proceedings of the CIMAC congress (paper no. 121), Bergen, Norway, 2010.

[5] D. Abbott, Hydrogen without tears: Addressing the global energy crisis via a solar to hydrogen pathway, Proc. IEEE 97 (2009) 1931–1934.

[6] D. Abbott, Keeping the energy debate clean: How do we supply the world's energy needs?, Proc. IEEE 98 (2010) 42–66.

[7] S. Verhelst, T. Wallner, Hydrogen-fueled internal combustion engines, Progress in Energy and Combustion Science 35 (6) (2009) 490–527.

[8] R. Sierens, S. Verhelst, Influence of the injection parameters on the efficiency and power output of a hydrogen fueled engine, Journal of Engineering for Gas Turbines and Power-Transactions of the ASME 125 (2) (2003) 444–449.

[9] S. Verhelst, P. Maesschalck, N. Rombaut, R. Sierens, Increasing the power output of hydrogen internal combustion engines by means of supercharging and exhaust gas recirculation, International Journal of Hydrogen Energy 34 (10) (2009) 4406–4412.

[10] S. Verhelst, P. Maesschalck, N. Rombaut, R. Sierens, Efficiency comparison between hydrogen and gasoline, on a bi-fuel hydrogen/gasoline engine, International Journal of Hydrogen Energy 34 (5) (2009) 2504–2510.

[11] S. Verhelst, J. Demuynck, R. Sierens, P. Huyskens, Impact of variable valve timing on power, emissions and backfire of a bi-fuel hydrogen/gasoline engine, International Journal of Hydrogen Energy 35 (9) (2010) 4399–4408.

[12] S. Verhelst, R. Sierens, A quasi-dimensional model for the power cycle of a hydrogen-fuelled ICE, International Journal of Hydrogen Energy 32 (15) (2007) 3545–3554.

[13] W. Annand, Heat transfer in the cylinders of reciprocating internal combustion engines, Proc Instn Mech Engrs 177 (36) (1963) 973–996.

[14] G. Woschni, A universally applicable equation for the instantaneous heat transfer coefficient in the internal combustion engine, SAE paper 670931 (1967).

[15] J. Demuynck, N. Raes, M. Zuliani, M. De Paepe, R. Sierens, S. Verhelst, Local heat flux measurements in a hydrogen and methane spark ignition engine with a thermopile sensor, International Journal of Hydrogen Energy 34 (24) (2009) 9857–9868.

[16] G. Wheeler, ASTM Manual for Rating Motor Fuels by Motor and Research Methods, 5th Edition, Baltimore, 1964.

[17] J. Taylor, An introduction to error analysis: the study of uncertainties in physical measurements, University Science Books, 1982.

[18] Vatell, Heat flux microsensor manual (2010).
URL `http://www.vatell.com/hfm.htm`

[19] J. Demuynck, M. De Paepe, R. Sierens, S. Verhelst, Heat transfer comparison between methane and hydrogen in a spark ignited engine, in: World Hydrogen Energy Conference, Essen, Germany, 2010.

[20] G. Borman, K. Nishiwaki, Internal-combustion engine heat-transfer, Progress in Energy and Combustion Science 13 (1) (1987) 1–46.

[21] W. Kleinschmidt, Instationäre Wärmeübertragung in Verbrennungsmotoren: Theorie, Berechnung und Vergleich mit Versuchsergebnissen, Fortschr.-Ber. VDI Reihe 12 nr. 383, VDI Verlag, DÃŒsseldorf, 1999.

[22] H. Pfriem, Der wärmeübergang bei schnellen druckänderungen in gasen besonders in versuchseinrichtungen zur messung des zündverzuges, Forschung auf dem Gebiete des Ingenieurwesens 13 (4) (1942) 150–164.

[23] K. Elser, Instationäre wärmeübertragung bei periodisch adiabater verdichtung turbulenter gase, Forschung auf dem Gebiete des Ingenieurwesens 21 (3) (1955) 65–74.

[24] W. Annand, Instantaneous heat transfer rates to the cylinder head surface of a small compression-ignition engine, Proc Instn Mech Engrs 185 (72) (1971) 976–987.

[25] G. Woschni, Beitrag zum problem des warmeuberganges im verbrenningsmotor, Motortechnische Zeitschrift 26 (4) (1965) 128–133.

[26] G. Sitkei, G. Ramanaiah, Rational approach for calculation of heat transfer in diesel engines, SAE paper 720027 (1972).

[27] G. Hohenberg, Advanced approaches for heat transfer calculations, SAE paper 790825 (1979).

[28] J. Chang, O. Guralp, Z. Filipi, D. Assanis, New heat transfer correlation for an HCCI engine derived from measurements of instantaneous surface heat flux, SAE paper 2004-01-2996 (2004).

[29] T. Shudo, H. Suzuki, Applicability of heat transfer equations to hydrogen combustion, JSAE Review 23 (3) (2002) 303–308.

[30] A. Nefischer, M. Hallmannsegger, A. Wimmer, G. Pirker, Application of a flow field based heat transfer model to hydrogen internal combustion engines, SAE paper 2009-01-1423 (2009).

[31] R. Reid, J. Prausnitz, B. Poling, The properties of Gases and Liquids, McGraw-Hill Book Co., Singapore, 1988.

[32] IAPWS, Revised release on the IAPWS formulation 1985 for the thermal conductivity of ordinary water substance (2008).
URL `http://www.iapws.org`